Reaction Zone Thickness of Turbulent Premixed Flame

Kazuhiro Yamamoto, Yasuki Nishizawa and Yoshiaki Onuma
Department of Mechanical Engineering,
Toyohashi University of Technology
1-1 Hibarigaoka, Tempaku, Toyohashi, Aichi 441-8580, JAPAN

ABSTRACT

Usually, we use the flame thickness and turbulence scale to classify the flame structure on a phase diagram of turbulent combustion. The flame structure in turbulence is still in debate, and many studies have been done. Since the flame motion is rapid and its reaction zone thickness is very thin, it is difficult to estimate the flame thickness. Here, we propose a new approach to determine the reaction zone thickness based on ion current signals obtained by an electrostatic probe, which has enough time and space resolution to detect flame fluctuation. Since the signal depends on the flow condition and flame curvature, it may be difficult to analyze directly these signals and examine the flame characteristics. However, ion concentration is high only in the region where hydrocarbon-oxygen reactions occur, and we can specify the reaction zone. Based on the reaction zone existing, we estimate the reaction zone thickness. We obtain the thickness of flames both in the cyclone-jet combustor and on a Bunsen burner, compared with theoretically predicted value, the Zeldovich thickness. Results show that the experimentally obtained thickness is almost the same as the Zeldovich thickness. It is concluded that this approach can be used to obtain the local flame structure for modeling turbulent combustion.

Keywords : turbulent flame, premixed combustion, reaction zone thickness, ion probe.

INTRODUCTION

For modeling turbulent combustion, numerous studies have been made [1-11]. In these studies, several different flame regimes have been proposed to classify the flame structure with a phase diagram [5,6]. It is considered that if the smallest turbulent eddies have a size below the reaction zone thickness, these eddies might penetrate into the reaction zone to form a thickened flame with distributed reaction zone [1-6]. As a limit between so called flamelet regime with thin wrinkled flame fronts and distributed combustion regime with thickened flame fronts, the Klimov-Williams criterion has been proposed. However, some recent studies have pointed out the persistence of laminar-like flame structure even under highly turbulent conditions [12,13]. In the work of Buschmann et al. [14], it has been found that thermal flame-front structure is significantly thinned com-

pared with that of the laminar flame, which is contrary to the expectation of thickened flames. Mansour et al. [15] have observed thin reaction zone with relatively thick preheat zone in simultaneous two-dimensional CH-LIF/Rayleigh measurements. Then, the flame structure in turbulence is still in debate, and a new phase diagram may be needed to construct turbulent combustion regimes.

In previous studies, with a cyclone-jet combustor, we have investigated turbulent flame structure over a wide range of turbulent intensities, with u'/S_L exceeding 10 in a stationary jet flame [16,17]. We have observed the flame behavior with CCD camera and high-speed video camera. Temperature measurement has been conducted with a compensated thermocouple. Results show that, in relatively weak turbulent flow, the wrinkled laminar flame is formed. When the velocity exceeds 20-30 m/s, one continuous flame sheet is not observed and the PDF of temperature is no longer bimodal, which is the typical thermal structure of the wrinkled laminar flame. Although there are certain inherent uncertainties in temperature measurement, it could be considered that, in highly turbulent flow, the flame structure is different from that of the laminar flame due to the turbulent motion.

For conclusive discussion, we need further studies to detect the local flame structure with diagnostics of high spatial and temporal resolution. Since the flame fluctuates strongly in turbulent flow and its reaction zone thickness is less than 1 mm, it is difficult to obtain its thickness experimentally. Recently, by the drastic improvement of laser diagnostics, it has been possible to obtain the two-dimensional flame image directly [15, 18, 19]. However, since the system is huge and is not easy for setting, the availability is limited. It is necessary to discuss the local flame structure based on statistically enough data. Here, we use an electrostatic probe to characterize the flame structure, which has high time resolution ($10^{-7}\sim 10^{-8}$ s [20]) enough to follow the flame fluctuation even under highly turbulent conditions. In this study, we propose a new approach to determine the reaction zone thickness based on probability of reaction zone existing. Compared with the Zeldovich thickness, we discuss the reaction zone thickness of turbulent flames.

EXPERIMENTAL

Figure 1 shows a cyclone-jet combustor used in this study. It consists of a combustion chamber with a main jet nozzle and two cyclone nozzles for pilot flames to stabilize turbulent flames. The diameter of the main jet nozzle, d, is 12.7 mm. The height of a cyclone combustor is 23 mm and the exit diameter is 21 mm, with two cyclone nozzles of 2.4 mm i.d.. The fuel is propane. In the experiment, we vary the mean velocity of the main jet, U_m (< 15ms), and the equivalence ratio of the mixture, ϕ_m, with a fixed condition of pilot flames for U_p = 20 m/s and ϕ_p = 0.7. The experimental conditions belong to the laminar flamelet regime. For comparison, a Bunsen-type burner is also used with exit diameter of 22mm.

The laser tomography technique is applied to obtain the instantaneous flame structure. A Nd:YAG laser (Spectra-physics GCR-170) operating at ca. 450 mJ/pulse is used to produce laser sheet of 300 μm thickness. The duration of laser pulse is 6 ns. MgO particles are used as seeding particles [17]. The Mie-scattering image is recorded by a still camera.

A micro-electrostatic probe is used to char-

acterize the flame structure. It specifies the reaction region of high ion concentration where the ion-electron formation and recombination reactions occur. It consists of a platinum wire sensor of 0.1 mm in diameter and 0.5 mm long. The sensor is projected from a fine quartz tube over which a water-cooled tube is fitted for preventing the thermal dielectric breakdown. The potential drop across the load resistance is amplified to obtain ion current, which is stored in the computer.

RESULTS AND DISCUSSION

Appearance of Flames

First, the observed flame in the cyclone-jet combustor is shown. Figure 2(a) shows a direct photograph of the flame for U_m = 10 m/s and ϕ_m = 0.75. The exposure time is about 0.01 s. Here, Z represents the axial distance from the exit of the combustor. The flame motion is very rapid and the instantaneous flame structure is not clear.

Figure 2(b) shows the tomographic image. In our previous study, we have found that there are three regions in the Mie-scattering image [17]. The first region is that of high intensity of scattering, which indicates unburned gas region of low temperature. The second region is that of low intensity of scattering, which is burned gas region of high temperature. The third is surrounding air of no scattering. So far, we have obtained tomographic images for U_m = 5 to 30 m/s with fixed equivalence ratio. As seen in this figure, when the turbulence is relatively low (U_m < 15 m/s), the so-called wrinkled laminar flame is formed with one flame sheet.

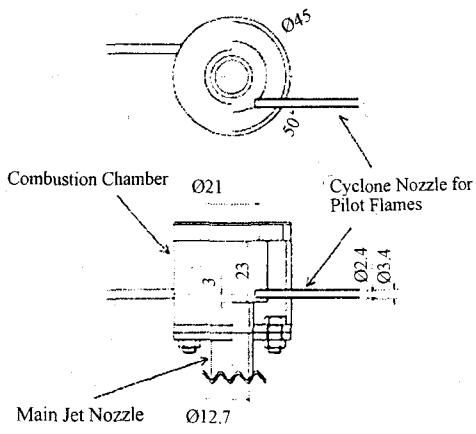

Fig. 1 Cyclone-jet combustor.

Figure 2(c) shows the axial distribution of mean ion current obtained along the center axis. The mean ion current becomes high around Z = 50~100 mm. Since the region of high ion current corresponds to the reaction region, it is considered that the flame is fluctuating within this region.

Signal Waveform and PDF of Ion Current

Next, we measure the ion current to characterize the flame. When the electrostatic probe passes the flame from the unburned gas side, the ion current starts to increase as a measuring point approaches the flame zone, and it reaches a maximum inside the reaction zone, then it decreases on the burned gas side. As already pointed out [8], the ion current in the burned gas is relatively high due to the slow recombination reaction. Figure 3(a) shows the signal waveforms of ion currents for U_m = 10 m/s and Z = 65 mm, where the mean ion current takes its maximum in the axial distribution (see Fig. 2(c)). The obtained ion current signal is largely fluctuating due to the flame motion.

Figure 3(b) shows the PDF profile of ion current at this position. More than 65,000 signal data are used. The number at the left

corner is the probability of zero ion current. It is well known that, when the turbulence is relatively weak, the so-called wrinkled laminar flame is formed and the PDF of temperature shows a bimodal shape, where two peaks of low and high temperatures correspond to those of the unburned and burned gases [17]. However, it is easily expected that its PDF of ion current is not bimodal, because the ion concentration is high only in the reaction zone, and the ion current is low in the unburned or burned gas regions. Even if the probe is inserted at the position where the reaction region more expectedly exits, both unburned and burned gases appear due to the flame fluctuation. Also, the reaction region is very thin. Then, the probability of high ion current is much lower, and the PDF profile in Fig.3(b) is observed for the wrinkled laminar flame.

Probability of Reaction Zone Existing and Reaction Zone Thickness

It should be noted that the ion current collected by an electrostatic probe depends on the flow velocity and flame curvature, and it difficult to derive the information of flames based only on the ion current signals [20]. However, at least, we can specify the reaction zone by examining the region of high ion concentration. In this study, we propose a new approach to determine the reaction zone thickness based on ion current signals statistically. Then, we can investigate the variations of the reaction zone thickness with turbulence quantitatively.

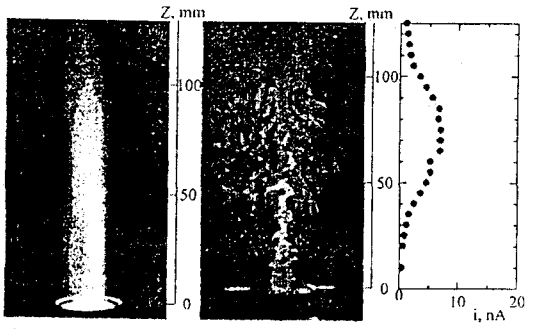

(a) Direct photograph (b) Tomographic image (c) Axial profile of ion current

Fig. 2 Flame in a cyclone-jet combustor, U_m = 10 m/s, Φ_m = 0.75

We explain the procedure briefly. Let us consider the example. We assume that the flame is stationary and the reaction zone is located between x = 0 and $x = \delta$, where x is the coordinate normal to the flame front, and δ is the reaction zone thickness. In this case, if we consider the probability of reaction zone existing, p, at specified location, it is unity inside the reaction zone, and zero outside the reaction zone. When we integrate $p(x)$ along x-axis, we can obtain the reaction zone thickness.

$$\int_{-\infty}^{+\infty} p(x)dx = \int_{0}^{\delta} p(x)dx$$

$$= \int_{0}^{\delta} 1\, dx = \delta$$

However, in turbulent flow, the flame is not stationary and always fluctuating. When the flame is inclined to integration axis, the reaction zone thickness is thicker. Therefore, the correction for flame inclination is needed. We take the coordinate normal to the mean flame surface, x^*. Assumed that the local flame structure is not affected by turbulence and reaction zone thickness does not change largely, this integration along the x^*-axis at this moment is,

$$\int_{-\infty}^{+\infty} p(x^*, t)dx^* = \delta^*(t) = \delta/\sin\theta,$$

where θ is the acute angle between the mean flame surface and the normal to the instantaneous flame front at a crossing point. By time-averaging procedure, the mean value of this

inclined reaction zone thickness becomes as follows:

$$\delta_m^* = \frac{1}{T}\int_0^T \delta^*(t)dt$$
$$= \frac{1}{T}\int_0^T \int_{-\infty}^{+\infty} p(x^*, t)dx^* dt.$$
$$= \int_{-\infty}^{+\infty} \frac{1}{T}\int_0^T p(x^*, t)dtdx^*.$$
$$= \int_{-\infty}^{+\infty} p_m dx^*,$$

where δ_m^* is the mean inclined reaction zone thickness, and T is the period of time averaging. Here, the variable with the subscript, *m*, is the time-averaged value. Since the flame is wrinkled and is not stationary, the averaged probability of reaction zone existing, p_m, is between zero and unity. By the correction of the inclination, we obtain the mean reaction zone thickness, δ_m.

$$\delta_m = \delta_m^* \times \overline{\sin\theta}$$
$$= \int_{-\infty}^{+\infty} p_m dx^* \times \overline{\sin\theta}$$

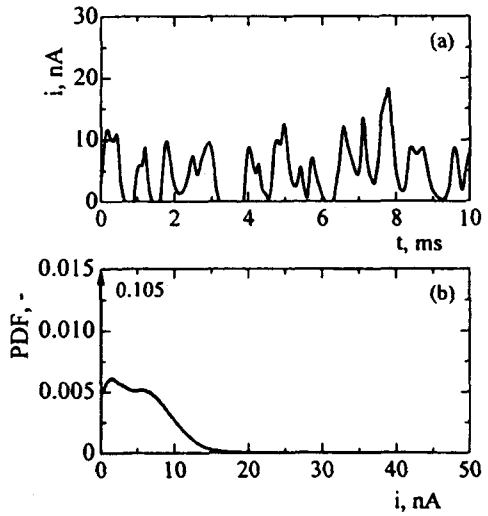

Fig. 3 (a) Signal waveform of ion current, (b) PDF of ion current; U_m=10m/s, Φ_m=0.75, Z=65mm.

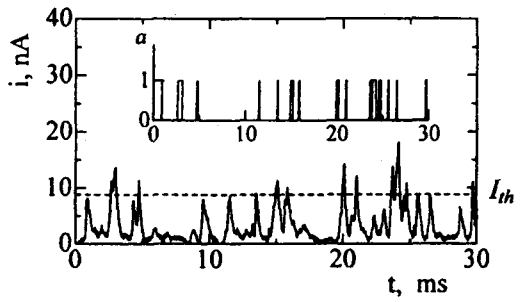

Fig. 4 Signal waveform of ion current and reaction variable,(U_m=15m/s, r=9mm, Z=20mm, ϕ_m=0.75)

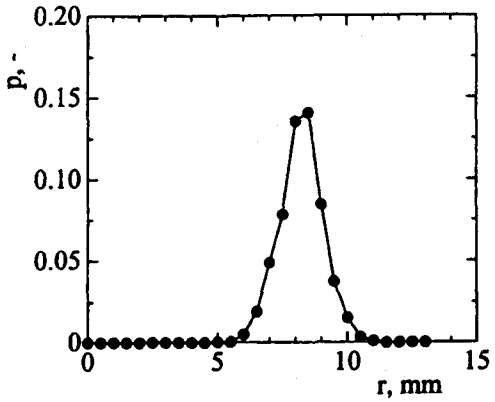

Fig. 5 Radial distribution of probability of reaction zone existing ; U_m=15m/s, Z=20mm, ϕ_m=0.75

Therefore, by determining the probability of reaction zone existing and the inclination angle experimentally, we can estimate the reaction zone thickness.

In Bray-Moss-Libby (BML) model [21], the inclination angle, θ, appears as the flamelet crossing angle, which is defined as the acute angle between the mean progress variable contour and the normal to the instantaneous front surface. In the work of Chew et al. [22], the overall mean cosine value of θ is found to be 0.5 for Bunsen flame. Based on over 200 tomographic images of flames formed in a cyclone-jet combustor, we confirmed that the mean cosine value of crossing angle is close to

0.5. Therefore, we correct the flame inclination by using this value.

To obtain the probability of reaction zone existing, $p_m(x^*)$, we need to know whether the reaction occurs or not at the specified time and space. We use simple threshold procedure. The ion current signals are binarized with reaction variable, a, whose value is unity or zero. This procedure is shown in Fig. 4 for U_m = 15m/s at r = 9 mm, Z = 20 mm. If the ion current is higher than the threshold, there occurs reaction and the reaction variable is unity, whereas if the ion current is lower than the threshold, a is zero. According to Okamoto et al. [20], the peak ion current across the flame depends on the angle between the flame and the sensor of the ion probe. Since ion current takes its maximum when the flame surface is parallel to the sensor, we adopt the half value of maximum ion current as threshold, I_{th}. Then, the width of half height is considered to be the time when the reaction zone passes the sensor. The lower peak value in Fig. 4 means the lower spatial resolution. We count the peaks only when the flame passes the sensor parallel to it. Otherwise, we may obtain the thickened flame due to the lower spatial resolution.

Next, we obtain the mean value of a by time-averaging procedure to determine the probability of reaction zone existing, p. Figure 5 shows the radial distribution of p for U_m = 15m/s at Z = 20 mm. As seen in this figure, the probability of reaction zone existing is high only at r = 6~10 mm, which means that the flame is fluctuating in this region. Based on tomographic images, the radial direction corresponds to the x^*-axis. By integration of p, we estimate the reaction zone thickness. Figure 6 shows the obtained reaction zone thickness for U_m = 5 m/s, Z = 10 mm as functions of equivalence ratio. The thickness of Bunsen flame (U = 1.8 m/s, ϕ = 0.85) is also shown. To confirm the validity of our method, we compare these values with the Zeldovich thickness, δ_z , which is obtained by $\delta_z \equiv \kappa / S_L$ [23,24], where κ is the thermal diffusivity of the mixture and S_L is the laminar burning velocity [25]. It is found that experimentally obtained values are very close to the Zeldovich thickness. It is concluded that, by our proposed method, the reaction zone thickness can be estimated correctly.

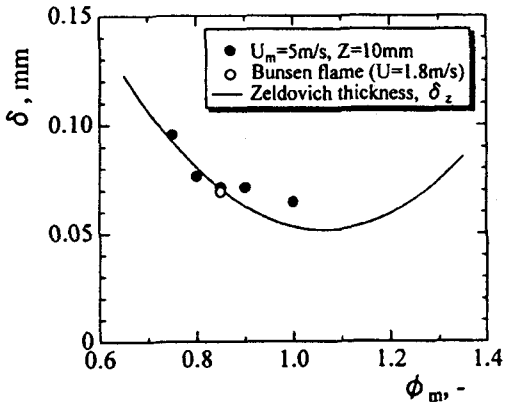

Fig. 4 Signal waveform of ion current and reaction variable,(U_m=15m/s, r=9mm, Z=20mm, ϕ_m=0.75)

CONCLUSIONS

By using the cyclone-jet combustor, the turbulent flame structure has been examined. With Mie scattering imaging, we have obtained tomographic images of flames. To detect flame fluctuation, we have used an electrostatic probe. Here, we have proposed a new approach to estimate the reaction zone thickness. We have obtained the reaction zone thickness of flames both in the cyclone-jet combustor and on a Bunsen burner, compared with the Zeldovich thickness. In our

experimental conditions, a typical wrinkled laminar flame is observed. The experimentally obtained thickness is almost the same as the Zeldovich thickness, which is reasonable for the laminar flamelet regime. It is concluded that this approach can be used to examine the local flame structure for modeling turbulent combustion.

REFERENCES

1. G. Damkoehler, *Z., Elektrochem.* 46, 1940, pp. 601-626.
2. D. R. Ballal and A. H. Lefebvre, *Proc. R. Soc. Lond. A.* 344, 1975, pp. 217-234.
3. M. Summerfield, S. H. Reiter, V. Kebely, and R. W. Mascolo, *Jet Propulsion* 25, 1955, p. 377.
4. K. N. C. Bray, Turbulent Reacting Flows, Topics in *Applied Physics*, 1980, Vol. 44, pp. 115-183.
5. R. Borghi, *in Recent Advances in Aeronautics Science*, 1985, pp. 117-134.
6. N. Peters, *21st Symp. (Int.) on Comb.*, 1986, pp. 1231-1250.
7. A. Yoshida, *22nd Symp. (Int.) on Comb.*, 1988, pp.1471-1478.
8. J. Furukawa, E. Harada, and T. Hirano, *23rd Symp. (Int.) on Comb.*, 1990, pp. 789-794.
9. A. Yoshida, M. Narisawa, and H. Tsuji, *24th Symp. (Int.) on Comb.*, 1992, pp. 519-525.
10. A. Yoshida. and K. Sakurai, *Transport Phenomena in Combustion*, 1995, pp. 509-520.
11. T. W. Lee and A. Mitrovic, *26th Symp. (Int.) on Comb.*, 1996, pp. 455-460.
12. Furukawa, J., Maruta, K., Nakamura, T., and Hirano, T., *Combustion Sci. Technol.* 90: 267-280 (1993).
13. Bedat, B. and Cheng, R. K., *Combus. Flame* 100: 485-494 (1995).
14. A. Buschmann, F. Dinkelacker, T. Schafer, and J. Wolfrum, *26th Symp. (Int.) on Comb.*, 1996, pp. 437-445.
15. M. S. Mansour, N. Peters, and Y. C. Chen, *27th Symp. (Int.) on Comb.*, 1998, pp. 767-773.
16. Y. Onuma, M. Morikawa, T. Takeuchi, and S. Noda, *Transport Phenomena in Combustion*, 1995, pp. 509-520.
17. K. Yamamoto, T. Achiha, and Y. Onuma, *AIAA Paper*, 2000-0186, 2000, pp.1-8.
18. Y. C. Cheng, and M. Mansour, *27th Symp. (Int.) on Comb.*, 1998, pp. 811-818.
19. F. Dinkelacker, A. Soika, D. Most, D. Hofmann, A. Leipertz, W. Polifke, and K. Dobbeling, *27th Symp. (Int.) on Comb.*, 1998, pp. 857-865.
20. K. Okamoto, J. Furukawa, and T. Hirano, *Nensyo no Kagaku to Gijutsu*, vol. 6, 1998, pp. 45-53.
21. Bray, K., N. C., Moss, J. B., and Libby, P. A., *Combust. Flame* 61:127-142 (1987).
22. Chew, T. C., Bray, K. N. C., and Britter, R., *Combust. Flame* 80:65-82 (1990).
23. Williams, F. W., *Combustion Theory*, 1985.
24. I. Gokalp, *Combust. Flame* 67:111-119 (1987).
25. I. Yamaoka and H. Tsuji, *20th Symp. (Int.) on Comb.*, 1984, pp. 1883-1892.